Molecular Pharmacology Fast Forward. Published on April 7, 2014 as doi: 10.1124/mol.114.092262

Differential effects of membrane cholesterol content on the transport activity of multidrug resistance-associated protein 2 (*ABCC2*) and of the bile salt export pump (*ABCB11*)

Christelle Guyot, Lia Hofstetter, Bruno Stieger

Department of Clinical Pharmacology and Toxicology University Hospital Zurich CH-8091 Zurich, Switzerland (C.G., L. H., S.S.)

Molecular Pharmacology Fast Forward. Published on April 7, 2014 as DOI: 10.1124/mol.114.092262
This article has not been copyedited and formatted. The final version may differ from this version.

Running Title

MRP2 and BSEP transport activity modulation by cholesterol

Corresponding author:

Bruno Stieger

University Hospital

Department of Clinical Pharmacology and Toxicology

Rämistrasse 100

8091 Zurich

Switzerland

Tel.: +41 44 255 20 68

Fax: +41 44 255 44 11

Email: bstieger@kpt.uzh.ch

Pages: 34

Table: 1

Figures: 8

References: 54

Abstract: 250 words

Introduction: 724 words

Discussion: 1489 words

Abbreviations:

ABC transporter, ATP binding cassette transporters; BSEP, bile salt export pump; CCK8, cholecystokinin 8; cLPM, canalicular plasma membrane; DTT, dithiothreitol; E17βG, estradiol-17-β-glucuronide; GSH, glutathione; MDR, multidrug resistance protein; MRP2, multidrug resistance-associated protein 2; OTA, ochratoxin A; PGE2, prostaglandin E2; RAMEB, randomly methylated-β-cyclodextrin.

Molecular Pharmacology Fast Forward. Published on April 7, 2014 as DOI: 10.1124/mol.114.092262
This article has not been copyedited and formatted. The final version may differ from this version.

Abstract

Rat canalicular membranes contain microdomains enriched in cholesterol and ATP-binding cassette transporters. Cholesterol is known to regulate the activity of transporters. Here, we investigated the effect of membrane cholesterol on the transport kinetics of MRP2 and of BSEP variants and mutants. MRP2 and BSEP were expressed with baculoviruses in insect cells, followed by vesicle isolation from control and cholesterol loaded (1mM cholesterol@RAMEB) cells for transport assays. We found that cholesterol stimulates MRP2 transport activity for substrates of different molecular weights: estradiol-17-β-glucuronide (E17βG), prostaglandin E_2 (PGE2), cholecystokinin 8 (CCK8) and vasopressin displayed an increase of V_{max} and a variable decrease of K_m. Kinetics of E17βG showed a sigmoidal shape and a mild cooperativity in Hanes-Woolf plots in control membranes. High cholesterol content shifted E17βG to Michaelis-Menten kinetics. PGE2/GSH transport followed Michaelis-Menten kinetics irrespective of cholesterol. The MRP2 substrates CCK8 and vasopressin exhibited Michaelis-Menten kinetics independent of membrane cholesterol content. Transport of ochratoxin A was ATP-dependent but neither mediated by MRP2 nor stimulated by cholesterol. Transport of the two most common BSEP variants p.444V/A showed Michaelis-Menten kinetics irrespective of membrane cholesterol, whereby cholesterol leads to an increased V_{max} while K_m remains unchanged. The transport activity of the BSEP mutants p.E297G and p.R432T increased at high cholesterol content but did not reach the capacity of normal BSEP. Hence, changing membrane cholesterol content modulates BSEP and MRP2 transport kinetics differently. Cholesterol increases the transport rates of BSEP and MRP2 but with the latter may also modify the binding site as e.g. for E17βG.

Molecular Pharmacology Fast Forward. Published on April 7, 2014 as DOI: 10.1124/mol.114.092262
This article has not been copyedited and formatted. The final version may differ from this version.

Introduction

Bile is constantly produced by the liver, contains a high concentration of bile salts and provides a route for hepatocellular elimination of poorly water soluble substances (Small, 2003). Bile salts and biliary phospholipids form mixed micelles, which protect the biliary system from the detergent action of bile salts (Trauner et al., 2008). Despite the partitioning of bile salts into mixed micelles, monomeric bile salt concentration in bile remains high (Roda et al., 1995). Since bile salts have detergent properties (Perez and Briz, 2009) and are cytotoxic (Utanohara et al., 2005), their high concentration can potentially damage the canalicular plasma membrane (cLPM). Furthermore, elevated concentrations of bile salts in hepatocytes impair hepatocellular functions.

Bile formation works against steep concentration gradients of solutes and therefore involves several ATP binding cassette (ABC) transporters (Small, 2003): bile salts are secreted by the bile salt export pump, (BSEP, *ABCB11*), which drives bile salt dependent bile flow and has a rather narrow substrate specificity (Stieger, 2011). The multidrug resistance-associated protein 2 (MRP2, *ABCC2*) transports a wide range of organic anions, mostly conjugates, which are the driving force for bile salt independent bile flow (Nies and Keppler, 2007). Phosphatidylcholine is translocated to the outer leaflet of the cLPM by multidrug resistance protein 3 (MDR3, *ABCB4*) (Oude Elferink and Paulusma, 2007) and cholesterol release from the cLPM is facilitated by the heterodimeric transporter ABCG5/ABCG8 (*ABCG5*, *ABCG8*) (Hazard and Patel, 2007).

We have recently demonstrated that cLPM contains detergent and bile salt resistant microdomains enriched in sphingomyelin and cholesterol, in which several ABC transporters, such as BSEP, MRP2 and MDR1 are located (Guyot and Stieger, 2011; Ismair et al., 2009). These microdomains may help protect the cLPM from solubilisation by bile salts. Cholesterol, which is enriched in microdomains, has been shown to modulate the activity of several ABC transporters like BSEP, MRP2, ABCG2 or MDR1 (Ito et al., 2008; Kimura et al., 2007a; Kis

Molecular Pharmacology Fast Forward. Published on April 7, 2014 as DOI: 10.1124/mol.114.092262
This article has not been copyedited and formatted. The final version may differ from this version.

et al., 2009; Telbisz et al., 2007). Partitioning of ABC transporters in and out of cholesterol rich microdomains could passively regulate the canalicular secretion of the respective substrates of these ABC-transporters.

The 3.8 Å structure of mouse Mdr1a reveals a large substrate binding pocket, explaining how Mdr1a is able to cope with a vast variety of compounds having a wide range of molecular weights (MW) (Aller et al., 2009). It was demonstrated that cholesterol stimulates MDR1 ATPase activity induced by small drugs (<500 Da), has no effect for ATPase activity stimulated by large drugs (800-900 Da) and suppresses ATPase activity induced by larger drugs (>1000 Da) (Kimura et al., 2007a). These findings suggest that the drug-binding site of MDR1 fits to drugs with a size of 800-900 Da and that cholesterol might support the recognition of smaller drugs by tightening the drug-binding site (Kimura et al., 2007b).

Similar to MDR1, MRP2 transports a large variety of substrates of largely different MW (Hirono et al., 2005). Hence, membrane cholesterol content may also differentially stimulate transport of small and large MRP2 substrates. On the other hand, BSEP has a much more restricted substrate specificity (Stieger, 2011; Stieger et al., 2007), which may lead to a different effect of membrane cholesterol content on its transport properties. Several dozen mutations in the *ABCB11* gene have been characterized in terms of expression and function. Often, BSEP function was studied in insect cells (Stieger, 2011), known for their very low cholesterol content (Gimpl et al., 1995), but the impact of membrane cholesterol on BSEP mutants awaits investigation. BSEP function may be inhibited by drugs (Dawson et al., 2012; Morgan et al., 2010; Stieger, 2010). We have presented evidence that the p.444A variant of BSEP, which constitutes the major polymorphic variant, is a susceptibility factor for drug and oestrogen induced cholestasis but is kinetically indistinguishable from the p.444V variant (Lang et al., 2007; Meier et al., 2008). While the two variants show similar kinetic properties, the p.444A variant tends towards lower protein levels in human liver (Meier et al., 2006). These two BSEP variants could potentially interact different with membrane cholesterol.

Molecular Pharmacology Fast Forward. Published on April 7, 2014 as DOI: 10.1124/mol.114.092262
This article has not been copyedited and formatted. The final version may differ from this version.

Therefore, we studied here the effect of cholesterol on transport activity and kinetic parameters of the two most common variants of BSEP and on two mutant forms of BSEP with decreased transport activity (Noe et al., 2005) and compared the effect of cholesterol on kinetic parameters of MRP2 assessed with low and high MW substrates.

Molecular Pharmacology Fast Forward. Published on April 7, 2014 as DOI: 10.1124/mol.114.092262
This article has not been copyedited and formatted. The final version may differ from this version.

Materials and Methods

Materials

Radiolabeled [^{3}H]estradiol-17-β-D-glucuronide (45 Ci/mmol), [^{3}H]taurocholic acid (4.6 Ci/mmol), [^{3}H]CCK8 (70 - 80.2 Ci/mmol), [5,6,8,11,12,14,15-^{3}H(N)]prostaglandin E_2 (181.7 – 200.0 Ci/mmol) and [phenlylalanyl-3,4,5-^{3}H(N)]vasopressin (8-L-arginine) (55.9 Ci/mmol) were purchased from PerkinElmer (Schwerzenbach, Switzerland). [^{3}H]ochratoxin A (10.6 – 26.0 Ci/mol) was obtained from PerkinElmer or from Movarek Biochemicals (Brea, CA). Cholecystokinin 8 (CCK8) was purchased from Bachem (Bubendorf, Switzerland), taurocholic acid sodium salt, estradiol-17-β-D-glucuronide (E17βG), ochratoxin A (OTA) and vasopressin were purchased from Sigma (St. Louis, MO). Prostaglandin E_2 (PGE2) was supplied by Cayman Chemicals (Ann Arbor, MI). Cholesterol complex of RAMEB (cholesterol@RAMEB) and RAMEB were purchased from Cyclolab (Budapest, Hungary). Purified polyclonal rabbit antibody against BSEP was described in (Noe et al., 2002), mouse monoclonal antibody against MRP2 (mAb (M2III-6)) was purchased from Enzo Life Science (Lausen, Switzerland). Horse radish peroxidase conjugated secondary antibodies were purchased from GE Healthcare (Little Chalfont, UK). Hank's Balanced Saline Solution (HBSS) was purchased from Gibco, Invitrogen, (Carlsbad, CA).

Transporter expression in Sf9 and Sf21 insect cells and membrane isolation

Human BSEP was expressed in Sf9 insect cells using the baculovirus system as described in (Noe et al., 2002). Human MRP2 was expressed in Sf21 insect cells using the baculovirus system as described in (de Waart et al., 2006). Membranes from insect cells expressing the different ABC-transporters were isolated as described in (Gerloff et al., 1998), resuspended in 50mM sucrose, 100mM KNO_3, 10mM HEPES/Tris pH 7.4 and stored in liquid nitrogen until use. Protein content was determined with the bicinchoninic acid method using a kit from Interchim (Montlucon, France).

Molecular Pharmacology Fast Forward. Published on April 7, 2014 as DOI: 10.1124/mol.114.092262
This article has not been copyedited and formatted. The final version may differ from this version.

Cholesterol loading

For cholesterol loading of infected Sf9 cells, we compared two different protocols. In the first protocol the loading was performed with intact cells as described in (Kis et al., 2009). Briefly cells were collected and treated for 30min at 37°C with ten times their volume of HBSS containing 1mM cholesterol@RAMEB. After 30min cells were washed in HBSS (in 20 times the initial volume). Membrane vesicle isolation from cholesterol loaded and mock treated virus-infected cells was performed as described above. The second loading protocol was performed with vesicles isolated as described in (Telbisz et al., 2007). Briefly, isolated vesicles were resuspended in cholesterol@RAMEB in 50mM sucrose, 100mM KNO_3, 10mM HEPES/Tris pH 7.4, at a final cholesterol concentration of 2mM and incubated at 37°C for 45min. After the incubation, cold buffer was added and vesicles were recovered by centrifugation and used for transport experiments. The efficiencies of the cholesterol loading and taurocholate transport activity of wild type BSEP expressing Sf9 cell vesicles are given in table 1.

Transport studies

ATP-dependent transport was determined by a rapid filtration technique as described in (Gerloff et al., 1998). Briefly, BSEP and MRP2 membrane vesicles (70µg protein) were incubated with 50mM sucrose, 100mM KNO_3, 12.5mM $Mg(NO_3)_2$, and 10mM HEPES/Tris pH 7.4, supplemented with [^{3}H]labeled and cold substrate at concentrations given in figure legends in presence or in absence of 5mM ATP. For CCK8 and vasopressin transport experiments, BSA was added to the uptake solution (to prevent proteolysis of the substrate) at 1mg/mL and to the cold stop solution at 10mg/mL to prevent non-specific filter binding. For the transport experiments with PGE2, GSH and DTT (5mM each) were added to the incubation solutions (de Waart et al., 2006), unless stated otherwise. For kinetic experiments, linearity of initial uptake rates as a function of time were determined in preliminary experiments (data not shown). All data were obtained from at least two independent

Molecular Pharmacology Fast Forward. Published on April 7, 2014 as DOI: 10.1124/mol.114.092262
This article has not been copyedited and formatted. The final version may differ from this version.

experiments (except for PGE2 kinetics) and are presented as mean ± S.D. for individual experiments. As the transporter expression levels varied to some extent between different membrane batches, only representative individual experiments are presented. Kinetic parameters were obtained by fitting initial uptake rates to the Michaelis-Menten equation by non-linear regression analysis with Prism 5 (GraphPad, San Diego, CA). The same program was used to transform and plot the data for the Hanes-Woolf plots (Neet, 1980).

Lipid determination and Western blotting

To assess cholesterol enrichment, lipids were extracted from isolated membrane vesicles as described in (Bligh and Dyer, 1959). Extracted lipids were analysed by thin layer chromatography for cholesterol amount as described in (Ismair et al., 2009). The amount of total phospholipids was determined as described in (Rouser et al., 1970). The lipid amounts were normalized to the amount of protein of the vesicles used for lipid extractions in order to be able to compare vesicles obtained from different isolations. To assess BSEP and MRP2 expression levels in cholesterol loaded and mock treated vesicles, 30µg of vesicles were processed by SDS-polyacrylamide electrophoresis and transferred to nitrocellulose membranes as described (Stieger et al., 1994). For detection of proteins, nitrocellulose membranes were blocked for 1h with 5% (wt/vol) non-fat dry milk dissolved in TBS-T (10mM Tris-HCl pH 7.6, 150mM NaCl, 0.1% (vol/vol) Tween20), incubated with primary antibodies in TBS-T for 2h at room temperature by three 10min washes in TBS-T. The blots were then incubated for 1h at room temperature with the appropriate secondary antibodies diluted in TBS-T/5%(wt/vol) dry milk, washed three times in TBS-T and developed with the UptiLight chemiluminesence reagent (Chemie Brunschwig, Basel, Switzerland).

Molecular Pharmacology Fast Forward. Published on April 7, 2014 as DOI: 10.1124/mol.114.092262
This article has not been copyedited and formatted. The final version may differ from this version.

Results

Since several protocols for membrane loading with cholesterol were available from literature, we decided to compare two of them. The cholesterol enrichment of membranes after loading and the effect of cholesterol loading on BSEP function were studied on Sf9 cells infected with BSEP (table 1). Cholesterol loading of intact cells or of isolated vesicles leads to an 8 fold increase in cholesterol content normalized to protein content. We observed a 2.2 and 1.5 fold increase in transport activity when the cholesterol loading was performed with intact cells (protocol 1) or isolated vesicles (protocol 2), respectively. The ATP-dependent transport after loading with the protocol 1 is considerably larger than after cholesterol loading with protocol 2. This may be explained by slightly different BSEP expression levels between different infections and more importantly by the stress put on the vesicles in protocol 2, which after their isolation went through additional incubations and high speed centrifugation. As consequence, we decided to use loading protocol 1 for further experiments. In order to test a potential impact of cholesterol loading on membrane lipid composition, total phospholipid content and cholesterol content of Sf9 and Sf21 vesicles was determined in three independent experiments. Control Sf9 cell vesicles contain 0.22 ± 0.021 μMol/mg total phospholipids and 0.020 ± 0.017 μMol/mg protein cholesterol, resulting in a phospholipid to cholesterol ratio of 16.0 ± 9.3. These values were in cholesterol loaded vesicles 0.33 ± 0.046 μMol/mg protein total phospholipids and 0.194 ± 0.187 μMol/mg protein cholesterol and a ratio of 1.9 ±1.2. Sf21 cell vesicles displayed a higher total phospholipid content, namely 0.493 ± 0.071 μMol/mg protein before and 0.529 ± 0.034 μMol/mg protein after cholesterol loading. The cholesterol content was 0.023 ± 0.012 μMol/mg protein before and 0.145 ± 0.033 μMol/mg protein after loading, resulting in a phospholipid to cholesterol ratio of 25.1 ± 11.1 before and 3.8 ± 0.7 after cholesterol loading. Hence, the total phospholipid content of the insect cell vesicles was not affected by cholesterol loading. Comparison of the total phospholipid content

Molecular Pharmacology Fast Forward. Published on April 7, 2014 as DOI: 10.1124/mol.114.092262
This article has not been copyedited and formatted. The final version may differ from this version.

of insect cell vesicles to published values for highly purified rat cLPM vesicles (0.83 μMol/mg protein (Meier et al., 1984), 0.67 μMol/mg protein (Bossard et al., 1993)) reveals that in rat cLPM the total phospholipid content is about twice the amount determined here in insect cell vesicles. Nevertheless, the total phospholipid to cholesterol ratio is comparable in insect cells after cholesterol loading to rat cLPM membrane vesicles reported (1.8 (Meier et al., 1984), 3.9 (Bossard et al., 1993)).

In order to study the effect of cholesterol on MRP2 transport activity, Sf21 cells infected with MRP2 were loaded with cholesterol as described in Material and Methods. Vesicles were analysed for MRP2 expression by Western blotting. Fig. 1A shows a representative Western blot of the cholesterol loaded and control vesicles demonstrating that cholesterol treatment had no effect on MRP2 expression level. Fig. 1B demonstrates that the cholesterol content is massively increased in membrane vesicles after cholesterol loading (0.413 ± 0.012 μMol cholesterol per mg protein n=8) compared to mock treated cells (0.038 ± 0.0017 μMol cholesterol per mg protein n=8) corresponding to an 11 fold increase of the specific cholesterol content. As MRP2 is transporting numerous substrates spanning a wide range of MW, we studied the effect of cholesterol on the transport of E17βG as a small substrate (MW 470) and of CCK8 as a large substrate (MW 1143). In contrast to others (Kopplow et al., 2005), we were not able to demonstrate MRP2-mediated estrone-3-sulfate (MW 372) transport in mock or cholesterol loaded Sf21 membrane vesicles (data not shown) confirming an earlier study (Sasaki et al., 2002). Fig. 1 shows that cholesterol loading has a marked effect on ATP-dependent transport of MRP2 expressing Sf21 cell vesicles: E17βG uptake was increased about 8 fold in presence of cholesterol (Fig. 1C) while CCK8 transport was increased about 6 fold in presence of cholesterol (Fig. 1D). It is interesting to note that E17βG uptake, but not CCK8 uptake was increased somewhat also in the absence of ATP after cholesterol loading (Fig. 1C versus Fig. 1D).

Molecular Pharmacology Fast Forward. Published on April 7, 2014 as DOI: 10.1124/mol.114.092262
This article has not been copyedited and formatted. The final version may differ from this version.

In order to distinguish between an effect of membrane cholesterol on the substrate affinity of MRP2 or on the turnover number, we next determined the kinetic parameters of E17βG and CCK8 transport by MRP2 (Fig. 2A-D) in the presence and absence of cholesterol loading. In absence of cholesterol loading, the uptake of E17βG as a function of substrate concentration was not consistent with classic Michaelis-Menten kinetics, but the plot showed the well-known sigmoidal shape (Bodo et al., 2003; Zelcer et al., 2003) (Fig.2A insert). This sigmoidal shape indicates a mild cooperativity, which is clearly displayed in the U-shaped Hanes-Woolf plot (Fig. 2E). Very interestingly, after loading with cholesterol, E17βG uptake versus substrate concentration shifted to classic Michaelis-Menten kinetics (Fig. 2B) leading to a linear Hanes-Woolf plot (Neet, 1980) (Fig. 2E). The loading with cholesterol leads to an increase in V_{max} (from 2214pmol/mg protein/min to 6673pmol/mg protein/min calculated for Fig. 2A and B) while the estimated low affinity K_m (581µM to 161µM) is decreased. As we encountered solubility problems for E17βG at concentrations higher than 1mM, this was the highest concentration used for the kinetic experiments. In contrast to E17βG, CCK8 transport by MRP2 showed a classic Michaelis-Menten behaviour with linear Hanes-Woolf plots at low and high membrane cholesterol content (Fig. 2C, D and F). The loading with cholesterol leads to an increase in V_{max} (from 269pmol/mg protein/min to 438pmol/mg protein/min calculated for Fig. 2C and D) while the K_m (27µM to 9µM) is decreased. Hence, cholesterol loading affects the kinetic parameters of MRP2 similarly for low and high MW substrates.

Next, we determined the kinetic parameters for MRP2 mediated vasopressin transport (Madon et al., 2000). As for CCK8, cholesterol consistently stimulated ATP-dependent vasopressin transport (data not shown). Kinetic analysis revealed a low affinity of vasopressin to MRP2, both in the absence and presence of cholesterol with high K_m-values (Fig. 3A): 315 µM in the absence of cholesterol and 103 µM in the presence of cholesterol. As for technical reasons no concentrations at values considerably higher than K_m could be used (data not shown) the estimation of the v_{max} values is subject to large uncertainty, but cholesterol loading increased

Molecular Pharmacology Fast Forward. Published on April 7, 2014 as DOI: 10.1124/mol.114.092262
This article has not been copyedited and formatted. The final version may differ from this version.

them (not shown). The corresponding Hanes-Woolf plots are shown in in Fig. 3B. Again, for this rather large MRP2 substrate (MW 1084), we found no evidence for cooperative kinetics in the absence or presence of cholesterol.

PGE2 is a substrate of MRP2 (de Waart et al., 2006) and has a MW of 353, which is comparable to the small substrate E17βG. Figure 4A shows that in the absence of cholesterol, PGE2 transport depends on the presence of GSH. If instead of GSH DTT was added, only a marginal MRP2-dependent PGE2 transport was observed (data not shown), indicating the GSH is needed as co-substrate for MRP2. In vesicles containing cholesterol, a marginal stimulation of transport was observed in the absence of GSH (Fig. 4A), which however was not in all experiments observed (data not shown). We conclude from this that cholesterol cannot replace GSH as co-substrate. Interestingly, however, cholesterol was able to stimulate PGE2 transport in the presence of GSH. First kinetic experiments indicated no saturation of PGE2 transport in the nM range (de Waart et al., 2006), irrespective of the presence of cholesterol. Consequently, we performed the kinetic analysis in the μM substrate range and found a large decrease of the Km value from 174 μM in the absence to cholesterol to 11.9 μM. The Hanes-Woolf plot in figure 4B shows that PGE2 transport did not display cooperativity neither in the absence nor in the presence of cholesterol. Due to the low affinity of this substrate for MRP2, the interpretation of the v_{max} values was not feasible.

OTA has been reported to be a MRP2 substrate (Leier et al., 2000), has a MW of 404 and was therefore considered to be an additional small MRP2 substrate. Interestingly, for this substrate we were not able to see a stimulation of transport activity by cholesterol (data not shown). Kinetic experiments pointed to OTA being a very low affinity substrate for MRP2 with no evidence for cooperativity in the corresponding Hanes-Woolf plot (Fig. 5A). Furthermore, the addition of GSH did not change its transport (Fig. 5B). We therefore also tested wild type Sf21 vesicles and found practically the same OTA transport activity as for vesicles isolated from MRP2 expressing cells, indicating that the observed ATP-dependent OTA transport is

Molecular Pharmacology Fast Forward. Published on April 7, 2014 as DOI: 10.1124/mol.114.092262
This article has not been copyedited and formatted. The final version may differ from this version.

due to an endogenous transporter in insect cells but not mediated by MRP2 (data not shown). In addition, we tested the effect of MK571 (an inhibitor of MRP2 and other MRPs, (Schrickx et al., 2006)) and of PSC833 (an inhibitor for MDR1 (Schrickx et al., 2006)) on OTA transport. We observed in MRP2 expressing Sf21 (and in control vesicles, data not shown) a weak inhibition a weak inhibition of OTA transport by MK571, but no inhibition by of PSC833 (Fig 5B) irrespective of the presence of GSH. This indicates that the observed endogenous OTA transport may be mediated by an MRP-like transporter in insect cells.

We next studied the effect of cholesterol on the transport activity of BSEP, which has a narrow substrate and size specificity (Stieger, 2011). Sf9 cells were infected with the two major BSEP isoforms (Pauli-Magnus et al., 2004), namely the p.444A and the p.444V variants, to determine the impact of membrane cholesterol on taurocholate transport activity. The conditions for infection of Sf9 cells with the two BSEP isoforms were adjusted such that comparable protein expression levels as shown by Western blotting were achieved in mock and cholesterol treated cells (Fig. 6A and D). The cholesterol loading of the membranes was comparable (Fig. 6B) for the two isoforms with an enrichment of about 11 fold (0.0292 μMol cholesterol per mg protein in mock treated vesicles compared to 0.307 μMol cholesterol per mg protein in cholesterol loaded vesicles). Fig. 6C and F show a comparable stimulation of the taurocholate transport activity of p.444A variant and p.444V variant after loading with cholesterol by 2.8 fold and 1.8 fold, respectively. Both BSEP isoforms show classic Michaelis-Menten kinetics and linear Hanes-Woolf plots (Fig. 7A and C) in the presence and absence of cholesterol, indicating the absence of cooperativity. This absence of cooperativity of taurocholate transport by BSEP in absence of cholesterol loading is in accordance with previous results obtained in our laboratory (Lang et al., 2007; Noe et al., 2005; Noe et al., 2002). The membrane loading with cholesterol leads to a marked increase in V_{max} (from 256pmol/mg protein/min to 579pmol/mg protein/min for p.444V and from 311pmol/mg protein/min to 447pmol/mg protein/min for p.444A, calculated for Fig. 7A and 7C) while the

Molecular Pharmacology Fast Forward. Published on April 7, 2014 as DOI: 10.1124/mol.114.092262
This article has not been copyedited and formatted. The final version may differ from this version.

K_m values (17µM to 25.3µM for p.444V and 13.5µM to 7µM for p.444A, calculated for Fig. 7A and 7C) remain unchanged in all experiments, irrespective of the isoform. The analysis of the kinetic parameters of the two BSEP variants by Hanes-Woolf transformations of the respective data at high and low cholesterol show lines of comparable slopes and y-axis intercepts (see example in Fig. 7B and 7D) corresponding to a classic Michaelis-Menten behaviour.

Finally, we studied the effect of cholesterol on two mutant forms of BSEP p.E297G and p.R432T found in patients with BSEP deficiency syndromes. These two mutants were previously shown to have a dramatically decreased transport activity (Noe et al., 2005). Western blot analysis detected comparable protein amounts for p.444A, p.297G and p.432T expressed in Sf9 vesicles (Fig. 8A, D and G) and a comparable amount of cholesterol after loading (Fig. 8B, E and H). As expected, the two mutants display in a low cholesterol environment a clearly reduced transport activity as compared to the p.444A variant (Fig. 8C, F and I), which after cholesterol loading considerably increased (6 fold increase for p.E297G and 3 fold increase for p.R432T). However this increase was not sufficient to reach the transport activity of the p.444A BSEP variant.

Molecular Pharmacology Fast Forward. Published on April 7, 2014 as DOI: 10.1124/mol.114.092262
This article has not been copyedited and formatted. The final version may differ from this version.

Discussion

In the present work we have investigated the role of membrane cholesterol content on the kinetics of the two ABC transporters MRP2 and BSEP. The main finding is that membrane cholesterol content modifies transport kinetics of BSEP and MRP2 in different ways. The established protocol for cholesterol loading of insect cells increases the cholesterol content of isolated vesicles about 10-fold. Sf9 cell membranes are known for having much lower cholesterol contents than mammalian plasma membranes {Gimpl, 1995 #6298}. Hence they are a good model for studying the effect of increasing membrane cholesterol levels without the prior need for cholesterol depletion. In cholesterol loaded insect membrane vesicles, the ratio of total phospholipid to cholesterol is comparable to rat cLPM membrane vesicles allowing a cautious extrapolation of the present findings to transporters in cLPM.

We took advantage of the broad substrate specificity of MRP2 accepting low MW (e.g. E17βG) and high MW (e.g. CCK8) substrates. At low membrane cholesterol, the kinetics of E17βG transport by MRP2 is sigmoidal yielding a U-shaped Hanes-Woolf plot. With cholesterol loaded membranes, the kinetics of E17βG transport follows Michaelis-Menten. This suggests a dependence of the allosteric properties of MRP2 for E17βG on membrane cholesterol. We tested PGE2 as another low MW substrate and found its transport activity to depend on the presence of GSH, as previously published (de Waart et al., 2006). An earlier publication reported no PGE2 transport by MRP2 expressed in insect cells (Reid et al., 2003). As the latter study was performed without GSH, our data on GSH dependence of PGE2 transport are confirming these earlier findings. While cholesterol loading stimulated PGE2 transport by MRP2, we did not observe cooperativity for this small substrate irrespective of membrane cholesterol. Previously, an increased affinity of MRP2 for E17βG (without major modification of v_{max}) together with a shift from cooperative to Michaelis-Menten kinetics in presence of indomethacin and sulfanitran was reported (Zelcer et al., 2003). Our findings therefore confirm and extend this study, as cholesterol or GSH also abolish cooperativity of

Molecular Pharmacology Fast Forward. Published on April 7, 2014 as DOI: 10.1124/mol.114.092262
This article has not been copyedited and formatted. The final version may differ from this version.

MRP2 for small substrates. Here, membrane cholesterol increases the v_{max} for two substrates but only mildly changes the K_m. In contrast, when transporting the large substrates CCK8 and vasopressin, MRP2 does not display cooperativity irrespective of membrane cholesterol content. Cooperativity of MRP2 for E17βG kinetics was reported previously (Bodo et al., 2003; Zelcer et al., 2003) and was interpreted as two drug binding sites interacting cooperatively (Borst et al., 2006). The data with GSH/PGE2 transport support a model with two binding sites for small substrates. Taking together small and large substrates, the data suggest that the binding site of MRP2 may be rather large. In the case of small substrates, two substrate molecules may bind sequentially to or close to the binding site, leading to an allosteric behaviour of MRP2. The exact mechanism of the cholesterol mediated activation of MRP2 transport activity is not evident. Currently, two possible mechanisms can be envisioned. The crystal structure of the Na,K-ATPase from shark rectal gland displays a cholesterol molecule, which is tightly bound to the membrane helix M7 and carried along from the native tissue (Shinoda et al., 2009). The activity of Na,K-ATPase strongly dependens on cholesterol (Cornelius et al., 2001). Cholesterol could similarly activate MRP2. This concept is supported by recent findings on ABCG2, where mutations of Arg482, residing in or very close to the third transmembrane helix, abolished cholesterol stimulation (Telbisz et al., 2014). Alternately, cholesterol could interact with the binding site(s) of MRP2. This concept was put forward for the ABC-transporter MDR1 with a very broad specificity for substrates of largely differing MW. The affinity of MDR1 substrates with low MW is increased by cholesterol, while the affinity for high MW substrates is cholesterol independent (Kimura et al., 2007a). To explain this difference, a cholesterol fill-in model for substrate recognition of MDR1 and other ABC transporters like ABCG1, ABCA1 or MDR2 was developed: part of the binding pocket is, if space allows, occupied by cholesterol (Kimura et al., 2007b). Indeed, a crystal structure of mouse p-glycoprotein at 3.8 Å reveals a large substrate binding area compatible this concept (Aller et al., 2009). From our results, it is

Molecular Pharmacology Fast Forward. Published on April 7, 2014 as DOI: 10.1124/mol.114.092262
This article has not been copyedited and formatted. The final version may differ from this version.

tempting to speculate that a similar mechanism may apply for some substrates of MRP2. In further support of this concept, bile salts have been shown to stimulate the transport activity of MRP2 (Bodo et al., 2003). Bile salts are synthesized from cholesterol and retain the 4-ring structure of cholesterol. Hence, they could bind at the same site as cholesterol to MRP2 and stimulate its transport activity. Also E17βG is derived from cholesterol retaining the 4-ring element of cholesterol. Taken together, the binding site for bile salts, cholesterol or the second E17βG molecule could adopt molecules having the 4-ring element of cholesterol. Importantly, our data together with literature data demonstrate that the transport mechanism of MRP2 for small substrates depends on the individual substrate, thus precluding a general transport mechanism for small MRP2 substrates, while larger substrates, based on our two examples, may share a common transport mechanism.

We also tested transport of OTA, previously reported to be a substrate of MRP2 (Leier et al., 2000), but found no MRP2 mediated OTA transport. The observed endogenous OTA transport in insect cell vesicles was subject to weak inhibition by MK571 but not by PSC833, suggesting that the endogenous transporter may belong to the ABCC family. Indeed, arthropods have genes belonging to the ABCC family (Dermauw and Van Leeuwen, 2013) and DMRP, which is the *Drosophila melanogaster* orthologue of the so-called "long" human MRPs displays typical transport characteristics of human MRPs (Szeri et al., 2009). As we were not able to stimulate the OTA transport activity by cholesterol, it is tempting to speculate that invertebrate ABC transporters may be cholesterol insensitive.

Cholesterol is known to stimulate the transport activity of BSEP (Kis et al., 2009; Paulusma et al., 2009). BSEP displays a considerably narrower substrate specificity than MRP2 and hence we investigated the effect of cholesterol on BSEP variants and mutants. The *ABCB11* gene coding for BSEP occurs with various polymorphic variants (Pauli-Magnus et al., 2004; Stieger, 2011). The most common single nucleotide polymorphism is c.1331T>C (p.444A) tending towards lower protein expression levels (Meier et al., 2006; Pauli-Magnus et al.,

Molecular Pharmacology Fast Forward. Published on April 7, 2014 as DOI: 10.1124/mol.114.092262
This article has not been copyedited and formatted. The final version may differ from this version.

2004). The c.1331C variant is a susceptibility factor for drug induced cholestasis and intrahepatic cholestasis of pregnancy (Pauli-Magnus et al., 2010), while the taurocholate transport kinetics of both variants are indistinguishable (Lang et al., 2007). Here, p.444V and p.444A showed an increased transport activity and a classic Michaelis-Menten behaviour after cholesterol loading but lacked cooperativity irrespective of cholesterol content (Fig. 4). We therefore conclude that cholesterol dependence of the two major BSEP variants does not constitute an additional susceptibility factor for acquired forms of cholestasis. The two investigated BSEP mutants were responsive to cholesterol loading. Compared to MRP2, kinetic experiments with BSEP are more challenging due to the toxic action of high bile salt concentrations, which inflict the integrity of membranes (Guyot and Stieger, 2011). The mutant forms of BSEP also showed an increase in v_{max} after cholesterol loading (data not shown). However this increase was not sufficient to restore the transport activity to levels comparable to the wild type isoforms. Consequently, data obtained from the *in vitro* characterization of BSEP mutants in the insect cells are valid to extrapolate to phenotypes of BSEP in mammalian membranes. This is further supported by the observation that inhibition of ATP-dependent taurocholate transport into rat cLPM vesicles and of rat Bsep expressed in Sf9 cells without cholesterol loading yields comparable inhibition constants (Stieger et al., 2000). While BSEP is a member of the B-family of ABC-transporters and a close relative of ABCB1 and transports low MW substrates, it does not display cooperativity as does ABCB1. The exact mechanism of the cholesterol effect(s) on transport activity will require the determination of the crystal structure of MRP2 and BSEP, which to date has not yet been accomplished. The cLPM of rats (and likely of humans) contains microdomains, which are enriched in cholesterol and contain rMRP2 and rBSEP (Guyot and Stieger, 2011; Ismair et al., 2009). Partitioning (modulated by canalicular bile salt concentration) of ABC transporters into microdomains may enhance their activity and constitute a regulatory mechanism in cLPM. Comparison of the extent of stimulation of MRP2 and BSEP reveals that the latter is

Molecular Pharmacology Fast Forward. Published on April 7, 2014 as DOI: 10.1124/mol.114.092262
This article has not been copyedited and formatted. The final version may differ from this version.

much less stimulated by increased membrane cholesterol. Consequently, the stimulation of these two transporters after partitioning into microdomains may differ.

In conclusion, we have shown that susceptibility of MRP2 and BSEP to cholesterol stimulation differs. Cholesterol increases the transport rates of BSEP and MRP2. However, for MRP2 but not BSEP, cholesterol may modify the binding of individual substrates. Therefore, transport properties of BSEP, like for example potential inhibition by drugs or drug metabolites are most likely less dependent on the expression system than the transport properties of MRP2. Hence, characterization of MRP2 may warrant the utilization of more than one expression system.

Molecular Pharmacology Fast Forward. Published on April 7, 2014 as DOI: 10.1124/mol.114.092262
This article has not been copyedited and formatted. The final version may differ from this version.

Authorship Contributions.

Participated in research design: Guyot, Stieger
Conducted experiments: Guyot, Hofstetter
Performed data analysis: Guyot, Hofstetter, Stieger
Wrote or contributed to writing of the manuscript: Guyot, Hofstetter, Stieger.

References

Aller SG, Yu J, Ward A, Weng Y, Chittaboina S, Zhuo R, Harrell PM, Trinh YT, Zhang Q, Urbatsch IL and Chang G (2009) Structure of P-glycoprotein reveals a molecular basis for poly-specific drug binding. *Science* **323**(5922):1718-1722.

Bligh EG and Dyer WJ (1959) A rapid method of total lipid extraction and purification. *Can J Biochem Physiol* **37**(8):911-917.

Bodo A, Bakos E, Szeri F, Varadi A and Sarkadi B (2003) Differential modulation of the human liver conjugate transporters MRP2 and MRP3 by bile acids and organic anions. *J Biol Chem* **278**(26):23529-23537.

Borst P, Zelcer N and van de Wetering K (2006) MRP2 and 3 in health and disease. *Cancer Lett* **234**(1):51-61.

Bossard R, Stieger B, O'Neill B, Fricker G and Meier PJ (1993) Ethinylestradiol treatment induces multiple canalicular membrane transport alterations in rat liver. *J Clin Invest* **91**(6):2714-2720.

Cornelius F, Mahmmoud YA and Christensen HR (2001) Modulation of Na,K-ATPase by associated small transmembrane regulatory proteins and by lipids. *J Bioenerg Biomembr* **33**(5):415-423.

Dawson S, Stahl S, Paul N, Barber J and Kenna JG (2012) In Vitro Inhibition of the Bile Salt Export Pump Correlates with Risk of Cholestatic Drug Induced Liver Injury in Man. *Drug Metab Dispos* **40**(1):130-138.

de Waart DR, Paulusma CC, Kunne C and Oude Elferink RP (2006) Multidrug resistance associated protein 2 mediates transport of prostaglandin E2. *Liver Int* **26**(3):362-368.

Dermauw W and Van Leeuwen T (2013) The ABC gene family in arthropods: Comparative genomics and role in insecticide transport and resistance. *Insect Biochem Mol Biol* **45C**:89-110.

Gerloff T, Stieger B, Hagenbuch B, Madon J, Landmann L, Roth J, Hofmann AF and Meier PJ (1998) The sister of P-glycoprotein represents the canalicular bile salt export pump of mammalian liver. *J Biol Chem* **273**(16):10046-10050.

Gimpl G, Klein U, Reilander H and Fahrenholz F (1995) Expression of the human oxytocin receptor in baculovirus-infected insect cells: high-affinity binding is induced by a cholesterol-cyclodextrin complex. *Biochemistry* **34**(42):13794-13801.

Guyot C and Stieger B (2011) Interaction of bile salts with rat canalicular membrane vesicles: evidence for bile salt resistant microdomains. *J Hepatol* **55**(6):1368-1376.

Hazard SE and Patel SB (2007) Sterolins ABCG5 and ABCG8: regulators of whole body dietary sterols. *Pflugers Arch* **453**(5):745-752.

Hirono S, Nakagome I, Imai R, Maeda K, Kusuhara H and Sugiyama Y (2005) Estimation of the three-dimensional pharmacophore of ligands for rat multidrug-resistance-associated protein 2 using ligand-based drug design techniques. *Pharm Res* **22**(2):260-269.

Ismair MG, Hausler S, Stuermer CA, Guyot C, Meier PJ, Roth J and Stieger B (2009) ABC-transporters are localized in caveolin-1-positive and reggie-1-negative and reggie-2-negative microdomains of the canalicular membrane in rat hepatocytes. *Hepatology* **49**(5):1673-1682.

Ito K, Hoekstra D and van Ijzendoorn SC (2008) Cholesterol but not association with detergent resistant membranes is necessary for the transport function of MRP2/ABCC2. *FEBS Lett* **582**(30):4153-4157.

Kimura Y, Kioka N, Kato H, Matsuo M and Ueda K (2007a) Modulation of drug-stimulated ATPase activity of human MDR1/P-glycoprotein by cholesterol. *Biochem J* **401**(2):597-605.

Kimura Y, Kodan A, Matsuo M and Ueda K (2007b) Cholesterol fill-in model: mechanism for substrate recognition by ABC proteins. *J Bioenerg Biomembr* **39**(5-6):447-452.

Kis E, Ioja E, Nagy T, Szente L, Heredi-Szabo K and Krajcsi P (2009) Effect of membrane cholesterol on BSEP/Bsep activity: species specificity studies for substrates and inhibitors. *Drug Metab Dispos* **37**(9):1878-1886.

Kopplow K, Letschert K, Konig J, Walter B and Keppler D (2005) Human Hepatobiliary Transport of Organic Anions Analyzed by Quadruple-transfected Cells. *Mol Pharmacol* **68**:1031-1038.

Lang C, Meier Y, Stieger B, Beuers U, Lang T, Kerb R, Kullak-Ublick GA, Meier PJ and Pauli-Magnus C (2007) Mutations and polymorphisms in the bile salt export pump and the multidrug resistance protein 3 associated with drug-induced liver injury. *Pharmacogenet Genomics* **17**(1):47-60.

Leier I, Hummel Eisenbeiss J, Cui Y and Keppler D (2000) ATP-dependent para-aminohippurate transport by apical multidrug resistance protein MRP2. *Kidney Int* **57**(4):1636-1642.

Madon J, Hagenbuch B, Landmann L, Meier PJ and Stieger B (2000) Transport function and hepatocellular localization of mrp6 in rat liver. *Mol Pharmacol* **57**(3):634-641.

Meier PJ, Sztul ES, Reuben A and Boyer JL (1984) Structural and functional polarity of canalicular and basolateral plasma membrane vesicles isolated in high yield from rat liver. *J Cell Biol* **98**(3):991-1000.

Meier Y, Pauli-Magnus C, Zanger UM, Klein K, Schaeffeler E, Nussler AK, Nussler N, Eichelbaum M, Meier PJ and Stieger B (2006) Interindividual variability of canalicular ATP-binding-cassette (ABC)-transporter expression in human liver. *Hepatology* **44**:62-74.

Meier Y, Zodan T, Lang C, Zimmermann R, Kullak-Ublick GA, Meier PJ, Stieger B and Pauli-Magnus C (2008) Increased susceptibility for intrahepatic cholestasis of pregnancy and contraceptive-induced cholestasis in carriers of the 1331T>C polymorphism in the bile salt export pump. *World J Gastroenterol* **14**(1):38-45.

Morgan RE, Trauner M, van Staden CJ, Lee PH, Ramachandran B, Eschenberg M, Afshari C, Qualls CW, Jr., Lightfoot-Dunn R and Hamadeh HK (2010) Interference with Bile Salt Export Pump Function is a Susceptibility Factor for Human Liver Injury in Drug Development. *Toxicol Sci* **118**(2):485-500.

Neet KE (1980) Cooperativity in enzyme function: equilibrium and kinetic aspects. *Methods Enzymol* **64**:139-192.

Nies AT and Keppler D (2007) The apical conjugate efflux pump ABCC2 (MRP2). *Pflugers Arch* **453**(5):643-659.

Noe J, Kullak-Ublick GA, Jochum W, Stieger B, Kerb R, Haberl M, Mullhaupt B, Meier PJ and Pauli-Magnus C (2005) Impaired expression and function of the bile salt export pump due to three novel ABCB11 mutations in intrahepatic cholestasis. *J Hepatol* **43**(3):536-543.

Noe J, Stieger B and Meier PJ (2002) Functional expression of the canalicular bile salt export pump of human liver. *Gastroenterology* **123**(5):1659-1666.

Oude Elferink RP and Paulusma CC (2007) Function and pathophysiological importance of ABCB4 (MDR3 P-glycoprotein). *Pflugers Arch* **453**(5):601-610.

Pauli-Magnus C, Kerb R, Fattinger K, Lang T, Anwald B, Kullak-Ublick GA, Beuers U and Meier PJ (2004) BSEP and MDR3 haplotype structure in healthy Caucasians, primary biliary cirrhosis and primary sclerosing cholangitis. *Hepatology* **39**(3):779-791.

Pauli-Magnus C, Meier PJ and Stieger B (2010) Genetic determinants of drug-induced cholestasis and intrahepatic cholestasis of pregnancy. *Semin Liver Dis* **30**(2):147-159.

Paulusma CC, de Waart DR, Kunne C, Mok KS and Elferink RP (2009) Activity of the bile salt export pump (ABCB11) is critically dependent on canalicular membrane cholesterol content. *J Biol Chem* **284**(15):9947-9954.

Perez MJ and Briz O (2009) Bile-acid-induced cell injury and protection. *World J Gastroenterol* **15**(14):1677-1689.

Reid G, Wielinga P, Zelcer N, van der Heijden I, Kuil A, de Haas M, Wijnholds J and Borst P (2003) The human multidrug resistance protein MRP4 functions as a prostaglandin efflux transporter and is inhibited by nonsteroidal antiinflammatory drugs. *Proc Natl Acad Sci U S A* **100**(16):9244-9249.

Roda A, Cerre C, Fini A, Sipahi AM and Baraldini M (1995) Experimental evaluation of a model for predicting micellar composition and concentration of monomeric species in bile salt binary mixtures. *J Pharm Sci* **84**(5):593-598.

Rouser G, Fleischer S and Yamamoto A (1970) Two dimensional then layer chromatographic separation of polar lipids and determination of phospholipids by phosphorus analysis of spots. *Lipids* **5**(5):494-496.

Sasaki M, Suzuki H, Ito K, Abe T and Sugiyama Y (2002) Transcellular transport of organic anions across a double-transfected Madin-Darby canine kidney II cell monolayer expressing both human organic anion-transporting polypeptide (OATP2/SLC21A6) and Multidrug resistance-associated protein 2 (MRP2/ABCC2). *J Biol Chem* **277**(8):6497-6503.

Schrickx J, Lektarau Y and Fink-Gremmels J (2006) Ochratoxin A secretion by ATP-dependent membrane transporters in Caco-2 cells. *Arch Toxicol* **80**(5):243-249.

Shinoda T, Ogawa H, Cornelius F and Toyoshima C (2009) Crystal structure of the sodium-potassium pump at 2.4 A resolution. *Nature* **459**(7245):446-450.

Small DM (2003) Role of ABC transporters in secretion of cholesterol from liver into bile. *Proc Natl Acad Sci U S A* **100**(1):4-6.

Stieger B (2010) Role of the bile salt export pump, BSEP, in acquired forms of cholestasis. *Drug Metab Rev* **42**:437-445.

Stieger B (2011) The role of the sodium-taurocholate cotransporting polypeptide (NTCP) and of the bile salt export pump (BSEP) in physiology and pathophysiology of bile formation. *Handb Exp Pharmacol* **201**:205-259.

Stieger B, Fattinger K, Madon J, Kullak Ublick GA and Meier PJ (2000) Drug- and estrogen-induced cholestasis through inhibition of the hepatocellular bile salt export pump (Bsep) of rat liver. *Gastroenterology* **118**(2):422-430.

Stieger B, Hagenbuch B, Landmann L, Höchli M, Schroeder A and Meier PJ (1994) In situ localization of the hepatocytic Na^+/Taurocholate cotransporting polypeptide in rat liver. *Gastroenterology* **107**(6):1781-1787.

Stieger B, Meier Y and Meier PJ (2007) The bile salt export pump. *Pflugers Arch* **453**(5):611-620.

Szeri F, Ilias A, Pomozi V, Robinow S, Bakos E and Varadi A (2009) The high turnover Drosophila multidrug resistance-associated protein shares the biochemical features of its human orthologues. *Biochim Biophys Acta* **1788**(2):402-409.

Telbisz A, Hegedus C, Varadi A, Sarkadi B and Ozvegy-Laczka C (2014) Regulation of the Function of the Human ABCG2 Multidrug Transporter by Cholesterol and Bile Acids: Effects of Mutations in Potential Substrate and Steroid Binding Sites. *Drug Metab Dispos* **42**(4):575-585.

Telbisz A, Muller M, Ozvegy-Laczka C, Homolya L, Szente L, Varadi A and Sarkadi B (2007) Membrane cholesterol selectively modulates the activity of the human ABCG2 multidrug transporter. *Biochim Biophys Acta* **1768**(11):2698-2713.

Trauner M, Fickert P, Halilbasic E and Moustafa T (2008) Lessons from the toxic bile concept for the pathogenesis and treatment of cholestatic liver diseases. *Wien Med Wochenschr* **158**(19-20):542-548.

Utanohara S, Tsuji M, Momma S, Morio Y and Oguchi K (2005) The effect of ursodeoxycholic acid on glycochenodeoxycholic acid-induced apoptosis in rat hepatocytes. *Toxicology* **214**(1-2):77-86.

Zelcer N, Huisman MT, Reid G, Wielinga P, Breedveld P, Kuil A, Knipscheer P, Schellens JH, Schinkel AH and Borst P (2003) Evidence for two interacting ligand binding sites in

Molecular Pharmacology Fast Forward. Published on April 7, 2014 as DOI: 10.1124/mol.114.092262
This article has not been copyedited and formatted. The final version may differ from this version.

human multidrug resistance protein 2 (ATP binding cassette C2). *J Biol Chem* **278**(26):23538-23544.

Molecular Pharmacology Fast Forward. Published on April 7, 2014 as DOI: 10.1124/mol.114.092262
This article has not been copyedited and formatted. The final version may differ from this version.

Footnotes.

BS is supported by the Swiss National Science Foundation (SNF) grant # [310030_144195], by the SNF National Center of Competence in Research (NCCR) TransCure (University of Berne, Berne, Switzerland) and by the Novartis Foundation for Biomedical Research (Basel, Switzerland) [07C75].

Molecular Pharmacology Fast Forward. Published on April 7, 2014 as DOI: 10.1124/mol.114.092262
This article has not been copyedited and formatted. The final version may differ from this version.

Figure legends

Figure 1. Effect of cholesterol loading on MRP2 expression and transport activity. A: Western blot analysis of MRP2 expressing vesicles with and without cholesterol loading (30µg protein per lane), B: Cholesterol content in MRP2 expressing vesicles detected by thin layer chromatography, 50µL and 5µL of extracted lipids were loaded for non-loaded vesicles and vesicles loaded with cholesterol, respectively. C: Initial rate of E17βG uptake (10µM) for 5min by membrane vesicles isolated from MRP2 expressing Sf21 cells with and without cholesterol loading. D: Initial rate of CCK8 uptake (0.2µM) for 10min by membrane vesicles isolated from MRP2 expressing Sf21 cells with and without cholesterol loading. Uptake was measured in presence (white bars) or in absence of ATP (black bars) as described in material and methods, the difference in the presence and the absence of ATP is represented with grey bars. Values given are mean ±S.D. of triplicate measurements of a representative experiment.

Figure 2. Kinetics of ATP dependent uptake of E17βG (A, B and E) and CCK8 (C, D and F) by MRP2 in membrane vesicles isolated from Sf21 cells. Initial uptake rates are given as the difference of uptake in the presence and absence of ATP. A: Uptake in presence of increasing concentrations of E17βG without cholesterol loading. B: Uptake in presence of increasing concentration of E17βG after cholesterol loading. C: Uptake in presence of increasing concentration of CCK8 without cholesterol loading. D: Uptake in presence of increasing concentration of CCK8 after cholesterol loading. E: Corresponding Hanes-Woolf plots for E17βG transport with (squares) and without cholesterol loading (circles). F: Corresponding Hanes-Woolf plots for CCK8 transport with (squares) and without cholesterol loading (circles). A-D, values given are mean ±S.D. of triplicate measurements but in some cases error bars are smaller than the size of the symbol.

Figure 3. Kinetics of ATP dependent uptake of vasopressin by MRP2 in membrane vesicles isolated from Sf21 cells. A: Initial uptake rates in presence of increasing vasopressin concentrations without (circles) and with cholesterol (squares) loading. B: Corresponding

Molecular Pharmacology Fast Forward. Published on April 7, 2014 as DOI: 10.1124/mol.114.092262
This article has not been copyedited and formatted. The final version may differ from this version.

Hanes-Woolf plots without (circles) and with (squares) cholesterol loading. A, values are mean ± S.D. of quadruplicate determinations, but in some cases error bars are smaller than the size of the symbols.

Figure 4. Effect of cholesterol loading on MRP2 mediated PGE2 transport in the presence and absence of GSH. A: Uptake of 1μM PGE2 was determined for 30 min. in the absence or presence of 5 mM GSH in control and cholesterol loaded vesicles. Uptake was measured in presence (white bars) or in absence of ATP (black bars) as described in Material and Methods, the difference in the presence and the absence of ATP is represented with grey bars. Values given are mean ± S.D. of quadruplicate measurements of a representative experiment. B: Hanes-Woolf plot for ATP-dependent PGE2 transport without (circles) and with cholesterol loading (squares) at increasing concentrations of PGE2 under initial uptake rates. Values are means of quadruplicate determinations.

Figure 5. Kinetics of ATP dependent uptake of OTA by MRP2 in membrane vesicles isolated from Sf21 cells. A: Initial uptake rates in presence of increasing OTA concentrations without cholesterol loading (top). The initial uptake rates of increasing OTA concentrations with cholesterol loading are omitted for clarity of the figure as the values are too close to the values without cholesterol loading. Bottom: Corresponding Hanes-Woolf plots without (circles) and with (squares) cholesterol loading. B: Effect of MK571 (25 μM) and PSC (5 μM) in the presence and absence of 5 mM GSH on transport of 10 μM OTA after 1 min. incubation. Black bars: Uptake in absence of ATP, white bars uptake in presence of 5 mM ATP as described in Materials and Methods, gray bars: ATP-dependent transport. Values are mean ± S.D. of quadruplicate determinations, but in some cases error bars are smaller than the size of the symbols.

Figure 6. Effect of cholesterol loading on BSEP expression and transport activity. A, D: Western blot analysis of p.444A variant (A) and p.444V variant (D) expressing vesicles with and without cholesterol loading (30μg protein per lane). B, E: Cholesterol content in p.444A

Molecular Pharmacology Fast Forward. Published on April 7, 2014 as DOI: 10.1124/mol.114.092262
This article has not been copyedited and formatted. The final version may differ from this version.

variant (B) and p.444V variant (E) expressing vesicles detected by thin layer chromatography, 50µL and 5µL of extracted lipids were loaded for non-loaded vesicles and vesicles loaded with cholesterol, respectively. C, F: initial rate of taurocholate uptake (2.5µM) for 10min by membrane vesicles isolated from p.444A variant (C) and p.444V variant (F) expressing Sf9 cells with and without cholesterol loading. Uptake was measured in presence (white bars) or in absence of ATP (black bars) as described in Material and Methods, the difference of uptake in the presence and the absence of ATP is represented with grey bars. Values given are mean ±S.D. of triplicate measurements of a representative experiment.

Figure 7. Kinetics of ATP dependent uptake of taurocholate by BSEP p.444A variant (A and B) and p.444V variant (C and D) in membrane vesicles isolated from Sf9 cells. Initial uptake rates were determined in the presence and absence of ATP with and without cholesterol loading (squares and circles, respectively). ATP dependent uptake values represent the difference between uptake in absence and presence of ATP. A: p.444A variant uptake in presence of increasing concentration of taurocholate. B: Corresponding Hanes-Woolf plot. C: p.444V variant uptake in presence of increasing concentration of taurocholate. D: Corresponding Hanes-Woolf plot. A and C: values given are mean ±S.D. of triplicate measurements but in some cases error bars are smaller than the size of the symbol**.**

Figure 8. Comparison of the effect of cholesterol loading on p.E297G and p.R432T on transport activity with p.444A. A, D, G: Western blot analysis of p.444A variant (A), p.E297G (D) and p.R432T (G) mutant BSEP expressing vesicles with and without cholesterol loading (30µg protein per lane). B, E, H: Cholesterol content in p.444A variant (B) p.E297G (E) and p.R432T (H) mutant BSEP expressing vesicles detected by thin layer chromatography, 50µL and 5µL of extracted lipids were loaded for non-loaded vesicles and vesicles loaded with cholesterol respectively. C, F, I: Initial rate of taurocholate uptake (2.5µM) for 10min by membrane vesicles isolated from p.444A variant (C) p.E297G (F) and p.R432T (I) mutant BSEP expressing Sf9 cells with and without cholesterol loading. Uptake

Molecular Pharmacology Fast Forward. Published on April 7, 2014 as DOI: 10.1124/mol.114.092262
This article has not been copyedited and formatted. The final version may differ from this version.

was measured in presence (white bars) or in absence of ATP (black bars) as described in Material and Methods, the difference between values in the presence and the absence of ATP is represented with grey bars. Values of a representative experiment are given as mean ±S.D. of triplicate measurements.

Molecular Pharmacology Fast Forward. Published on April 7, 2014 as DOI: 10.1124/mol.114.092262
This article has not been copyedited and formatted. The final version may differ from this version.

Tables

Table 1. Comparison of different cholesterol loading protocols.

	Cholesterol content (µMol/mg protein)			Taurocholate transport for 10 min (pmol/mg protein)					
				No cholesterol loading			Cholesterol loading		
	No loading	Cholesterol loading	Fold increase	- ATP	+ ATP	Difference	- ATP	+ ATP	Difference
Protocol 1	0.0303	0.267	8.8	33.3	293.8	260.5	45.8	627.1	581.3
Protocol 2	0.0367	0.302	8.2	23.5	102.5	79.0	11.4	132.1	120.7

Taurocholate transport activity of wild type BSEP expressing Sf9 cell vesicles was determined after cholesterol loading with two different protocols. For each protocol, the cholesterol enrichment was calculated after lipid extraction and determination of cholesterol amount by thin layer chromatography. Transport experiments were realised as described in Material and Method. Cholesterol enrichment and transport studies were reproduced at least two times independently.

Figure 1

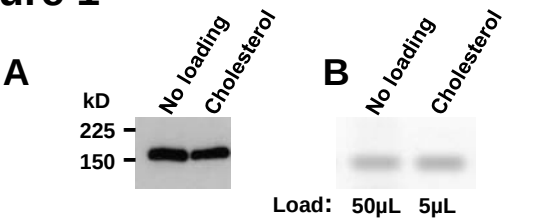
A
No loading
Cholesterol
kD
225
150
B
No loading
Cholesterol
Load: 50µL 5µL

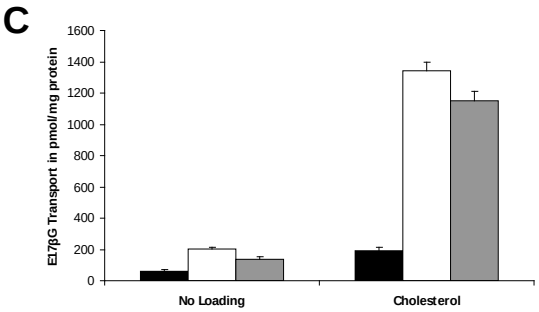
C
E17βG Transport in pmol/mg protein
1600
1400
1200
1000
800
600
400
200
0
No Loading
Cholesterol

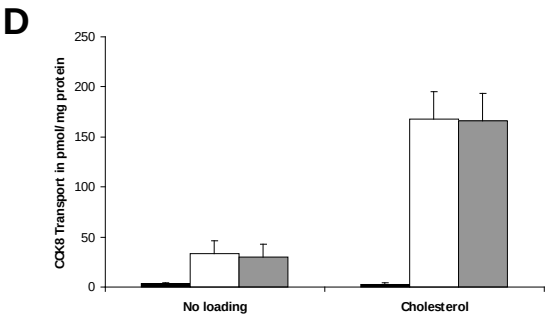
D
CCK8 Transport in pmol/ mg protein
250
200
150
100
50
0
No loading
Cholesterol

Figure 2

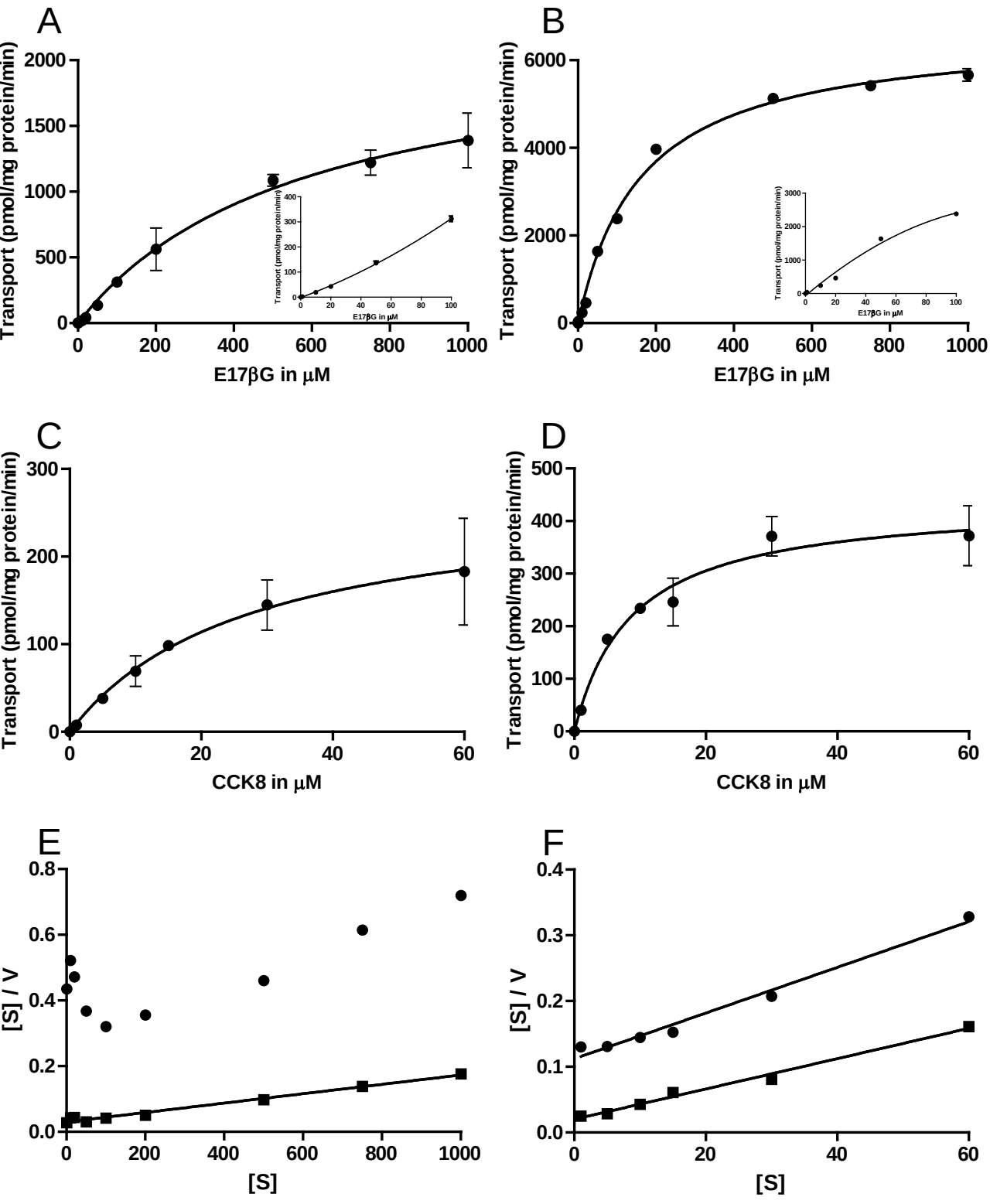
A
Transport (pmol/mg protein/min)
2000
1500
1000
500
0
0
200
400
600
800
1000
E17βG in μM
Transport (pmol/mg protein/min)
400
300
200
100
0
0
20
40
60
80
100
E17βG in μM
B
Transport (pmol/mg protein/min)
6000
4000
2000
0
0
200
400
600
800
1000
E17βG in μM
Transport (pmol/mg protein/min)
3000
2000
1000
0
0
20
40
60
80
100
E17βG in μM
C
Transport (pmol/mg protein/min)
300
200
100
0
0
20
40
60
CCK8 in μM
D
Transport (pmol/mg protein/min)
500
400
300
200
100
0
0
20
40
60
CCK8 in μM
E
[S] / V
0.8
0.6
0.4
0.2
0.0
0
200
400
600
800
1000
[S]
F
[S] / V
0.4
0.3
0.2
0.1
0.0
0
20
40
60
[S]

Figure 3

A

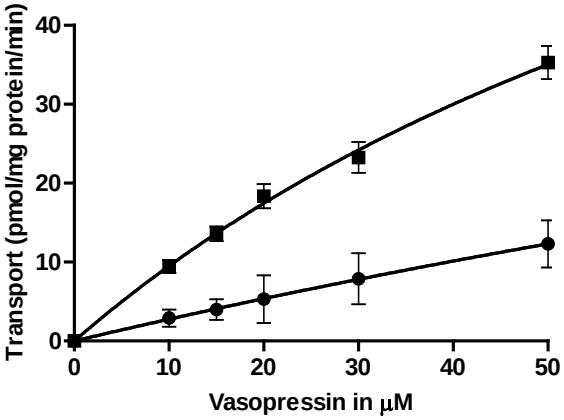
Transport (pmol/mg protein/min)
0
10
20
30
40
0
10
20
30
40
50
Vasopressin in µM

B

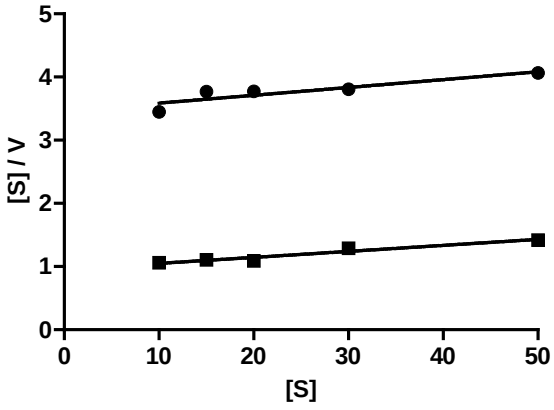
[S] / V
0
1
2
3
4
5
0
10
20
30
40
50
[S]

Figure 4

A

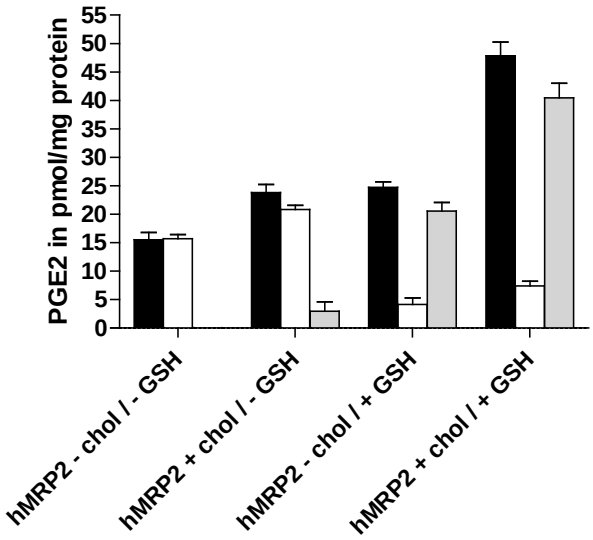
PGE2 in pmol/mg protein
55
50
45
40
35
30
25
20
15
10
5
0
hMRP2 - chol / - GSH
hMRP2 + chol / - GSH
hMRP2 - chol / + GSH
hMRP2 + chol / + GSH

B

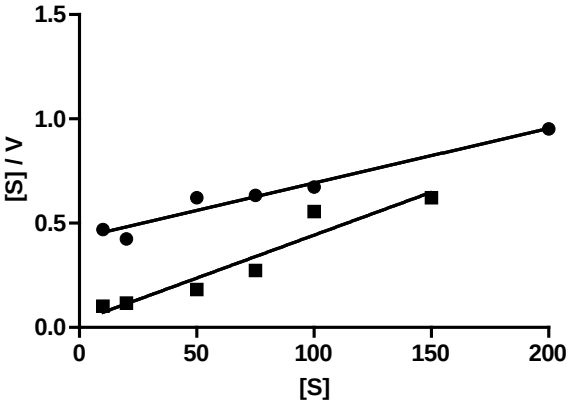
[S] / V
1.5
1.0
0.5
0.0
0
50
100
150
200
[S]

Figure 5

A

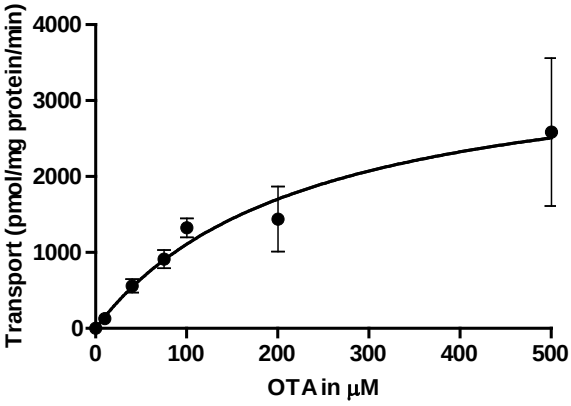
Transport (pmol/mg protein/min)
4000
3000
2000
1000
0
0
100
200
300
400
500
OTA in µM

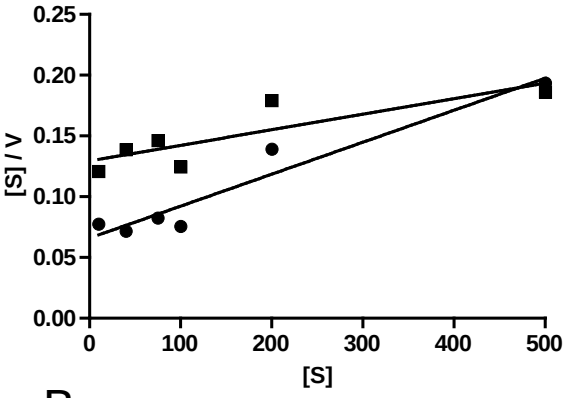
[S] / V
0.25
0.20
0.15
0.10
0.05
0.00
0
100
200
300
400
500
[S]

B

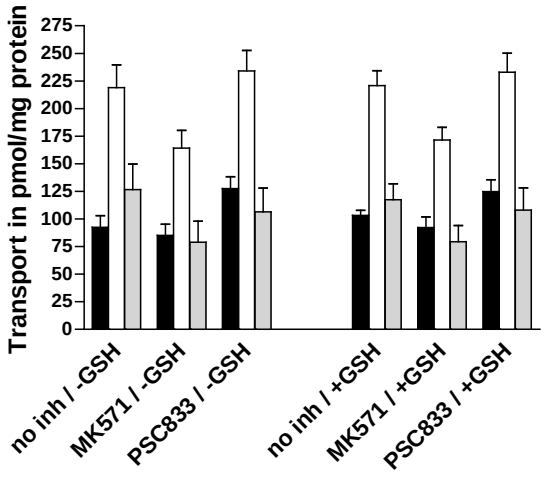
Transport in pmol/mg protein
275
250
225
200
175
150
125
100
75
50
25
0
no inh / -GSH
MK571 / -GSH
PSC833 / -GSH
no inh / +GSH
MK571 / +GSH
PSC833 / +GSH

Figure 6

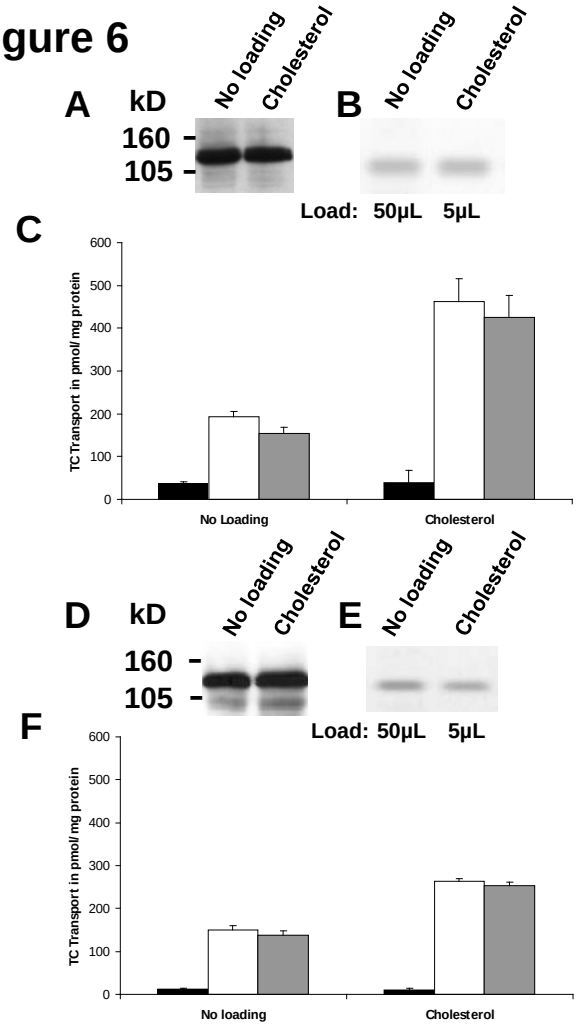
A
kD
No loading
Cholesterol
160
105
B
No loading
Cholesterol
Load: 50µL 5µL
C
TC Transport in pmol/ mg protein
600
500
400
300
200
100
0
No Loading
Cholesterol
D
kD
No loading
Cholesterol
160
105
E
No loading
Cholesterol
Load: 50µL 5µL
F
TC Transport in pmol/ mg protein
600
500
400
300
200
100
0
No loading
Cholesterol

Figure 7

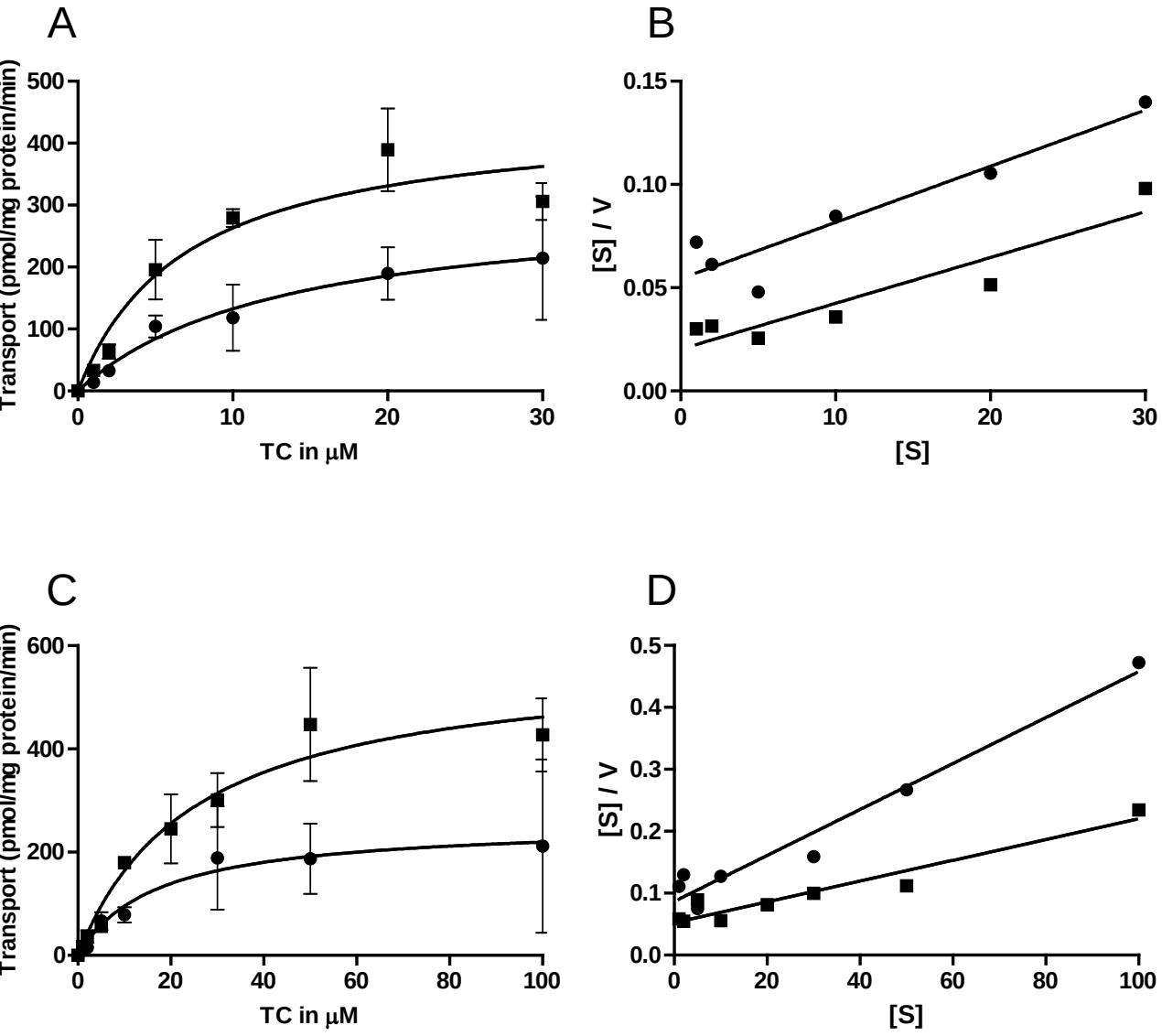
A
B
C
D
Transport (pmol/mg protein/min)
TC in μM
[S] / V
[S]
0
10
20
30
40
60
80
100
200
300
400
500
600
0.00
0.05
0.10
0.15
0.0
0.1
0.2
0.3
0.4
0.5

Figure 8

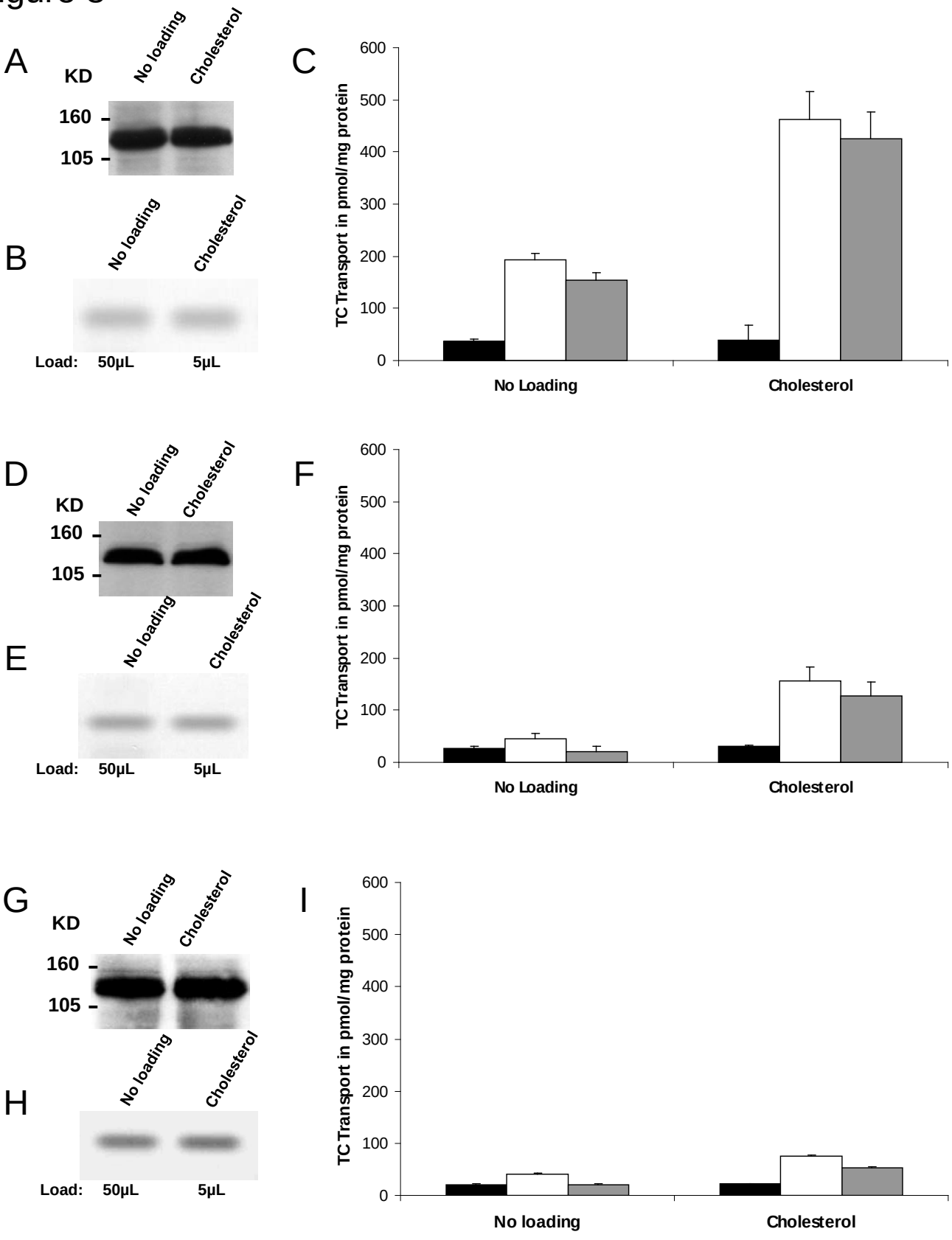
A
KD
No loading
Cholesterol
160
105
B
No loading
Cholesterol
Load: 50µL 5µL
C
TC Transport in pmol/mg protein
600
500
400
300
200
100
0
No Loading
Cholesterol
D
KD
No loading
Cholesterol
160
105
E
No loading
Cholesterol
Load: 50µL 5µL
F
TC Transport in pmol/mg protein
600
500
400
300
200
100
0
No Loading
Cholesterol
G
KD
No loading
Cholesterol
160
105
H
No loading
Cholesterol
Load: 50µL 5µL
I
TC Transport in pmol/mg protein
600
500
400
300
200
100
0
No loading
Cholesterol